

Use of A Commercial Wind SODAR for Measuring Wake Vortices

Stephen M. Mackey*

U.S. Department of Transportation, Volpe Center, Cambridge, MA 02142

David C. Burnham†

Scientific and Engineering Solutions, Inc., Orleans, MA 02653

This paper describes the application of a commercial wind SODAR (SO_Nic De_Tection And Ra_Nging) to the measurement of aircraft wake vortices. Changes in data collection and processing were required to extract vortex location and circulation from the acoustic returns. Sample data are presented, and it is demonstrated that SODARs represent valuable addition to the existing array of sensors for tracking and characterizing aircraft vortices in-ground effect.

I. Introduction

SODARS (then termed the Monostatic Acoustic Vortex Sensing System; fundamentally as a form of acoustic Radar) were used extensively in the 1970s to measure wake vortices, specifically for characterizing circulation and decay. Earlier and subsequent tests examined a variety of SODAR antenna configurations and the most successful was found to be a vertical antenna measuring acoustic back scattering¹. An array of SODAR antennas can track the lateral motion and decay of wake vortices as they pass over successive antennas. These early vortex SODAR used (a) separate horn-dish antennas for transmit and receive to avoid ringing and measure near the ground and (b) analog signal recording. Spectral analysis used expensive analog/digital spectrum analyzers controlled by a minicomputer. An upgraded sodar version was deployed in 1990 with digital recording and off-line processing using the Fast Fourier Transform (FFT).

Subsequent advances in technology have led to commercial wind SODAR with:

1. Phased-array antennas operating at higher frequencies (e.g., 4500 Hz versus 2950 and 3600 Hz used in the earlier vortex sodars) that (a) give better velocity resolution and (b) have negligible ringing so that a single antenna can be used to transmit and receive.
2. Modern data acquisition system that (a) include real-time Doppler processing and (b) can record the raw spectra and spectral moments.
3. Independent operation requiring only power and digital signal connection. (Note that cross interference between closely spaced SODAR could occur but can be mitigated by different operating frequencies.)

Wind SODARs are now commercially available from a number of vendors and they are designed to measure wind profiles from the ground to a specific maximum height above the ground that depends upon the operating frequency (and hence the amount of atmospheric attenuation). Site surveys for wind power application are perhaps the most frequent application. Also recently, for both environment and homeland security concerns, wind SODARs also been increasingly used to support these studies. Wind SODAR performance depends strongly on atmospheric conditions (amount of backscatter) and the ambient noise level. Wind profiling SODARs can be adapted to measure wake vortices with relatively small investment in software modification, signal processing and algorithm development. The purpose of this paper is to describe these methods and document the resulting vortex measurement capability. The use of wind SODARs for this purpose is very cost effective because most of the engineering required for a

* Electronics Engineer, Advanced CNS Technologies Division (RTV-4A), 55 Broadway, Cambridge, MA 02142.

† President, Scientific and Engineering Solutions, 16 Anchor Drive, Orleans, MA 02653, Senior Member AIAA.

vortex SODAR has already been incorporated in the design of a wind SODAR. It may also be noteworthy that the method of SODAR detection of wake vortices has also received renewed attention internationally.^{2,3}

II. SODAR Parameter Hardware Settings

A. Sodar Placement and Data Quantity

The SODARs deployed were the Atmospheric Systems Corporation Model 4000 (formally the Aerovironment MiniSodar 4000) Proper placement of several SODARs allows the monitoring of wakes as they decay in-ground effect (IGE), defined as a region where vortices are situated in a region whose height is approximately half that of the initial vortex spacing. The St. Louis Lambert International Airport has been the primary test site for the current joint FAA-NASA wake turbulence program since 2003,^{4,5} and the final configuration consisted of three SODARs spaced in an array parallel to one of the two arrays of crosswind propeller anemometers (otherwise known as a Windline, which tracks the vortex induced crosswinds), as well as along the scan plane of a *WindTracer*[®] pulsed LIDAR (Light Detection and Ranging, essentially a RADAR operating in optical frequencies, manufactured by Coherent Technologies Inc, - Currently Lockheed Martin Coherent Technologies), and located to best measure the wakes from arriving aircraft on runway 12R. As the wakes transport laterally, the SODAR array measured the disturbance and quantified the decay from the first SODAR as compared to the second and third SODARs.

SODAR array operations were conducted over the time period of February 04 to January 06. The case selected for this paper was measured from the SODAR closest to runway 12R. The vortex was produced from a Boeing 737 on October 22, 2005 at 12:53:43 PM UTC.

B. Parameter Settings

The SODAR adapted for wake vortex studies (a) is designed for a maximum altitude of 200 meters, (b) uses three beams (vertical and two orthogonal beams tilted 16 degrees from vertical) to measure vertical profiles of all three wind components with a range resolution of 5 meters, (c) operates with a typical pulse length of 70 msec, and (d) obtains a new wind profile every 4 seconds. In fact, the first wake vortex measurements with this sodar were obtained from wind measurements near the operating runways at SFO airport. A factor of 10 improvement in the update time (to 0.45 seconds) can be achieved by using only the vertical beam and reducing the maximum range to 60 meters this configuration can effectively measure wake vortices up to a height of 50 meters, which is adequate for studying wakes in-ground effect. The update time is important because the sodar generates a time series of vertical wind profiles that sample a wake vortex as it passes over the sodar antenna. For example, a vortex traveling at 5 m/s will have a very coarse sample spacing of 20 m for a 4-second update time but a much better sample spacing of 2.25 m for an update time of 0.45 seconds.

The preferred SODAR operating mode for vortex measurements is to record time series. The SODAR return signal is mixed with the transmit signal to generate in-phase (I) and quadrature (Q) signals that are band-pass filtered and sampled at 960 Hz. Time series recording has two advantages: (a) range-gate spacing can be defined after recording rather than in real time and (b) the return signal can be studied directly (e.g., to look at core reflections; see below). The SODAR return signal is mixed with the transmit signal to generate in-phase and quadrature signals that are band-pass filtered and sampled at 960 Hz. In vortex mode, the SODAR's transmit pulse length was set to 30 msec to improve the vertical resolution to approximately 5 m and to permit measurements close to the ground. The FFT length was set to 32 points (33.3 msec) to give comparable resolution to the pulse length.

III. Acoustic Back Scattering Process

The vortex signals detected by the SODAR are generated by three different mechanisms:

1. The most useful is scattering from the turbulence embedded in the vortex flow field. The Doppler shift from such scattering is characteristic of the flow velocity. Turbulence scattering depends upon wavelength matching; for backscattering the turbulence wavelength must be half that of the acoustic wave. Also, for backscattering, scattering occurs mostly from temperature fluctuations, not velocity fluctuations. This type of scattering leads to one of the serious limitations of wind SODARs; sometimes the level of thermal fluctuations in the atmosphere is very low and wind measurements are not reliable. Fortunately, wake vortices are always observed to have sufficient thermal fluctuations for good measurements; entrained engine exhaust is likely the source of these fluctuations.
2. If the pressure drop in the vortex core is great enough, it can generate a coherent, direct backscatter signal. If the vortex core is perpendicular to the acoustic beam, this signal can be much larger than

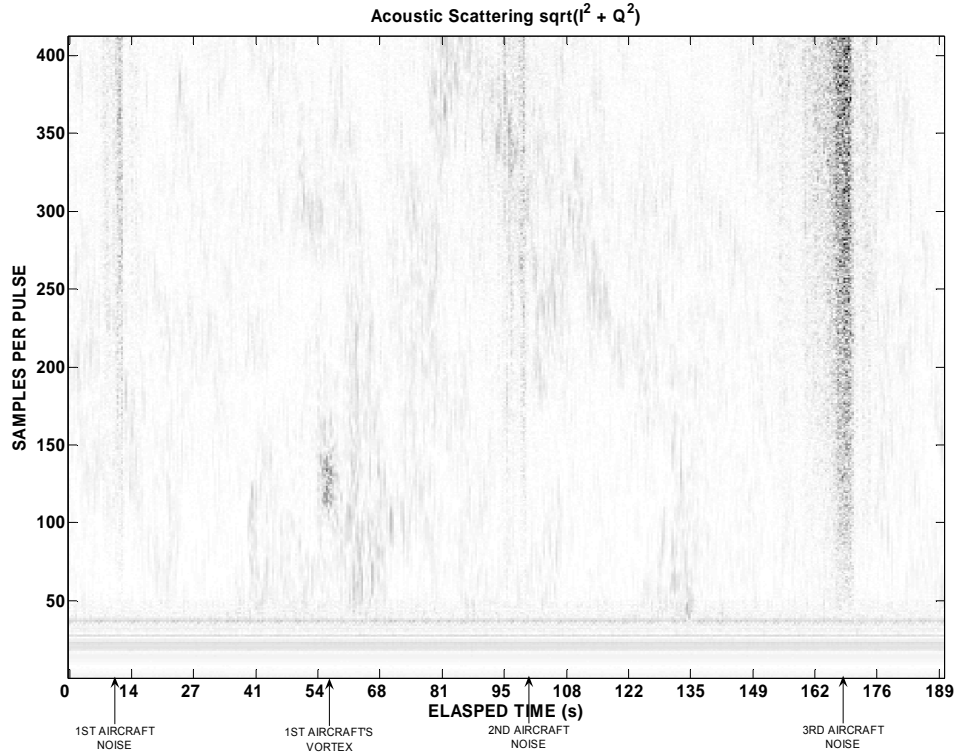


Figure 1 Acoustic Scattering Amplitude data for the vortex of a Boeing 737 landing at STL Airport.

turbulence scattering because the scattered signal spreads out in a plane, not all space. Core scattering is Doppler shifted by the vertical motion of the core as a whole, not the flow field in the core. Strong core scattering is evidence for a small vortex core size. However, the absence of core scattering is not evidence for a large core because the core might be tilted to scatter away from the SODAR antenna. A careful analysis of core scattering might give an indication of the core size, which, at present, is not readily obtained by any other ground-based or flight measurement methods.

3. Under some conditions a vortex core can generate noise in the operating band of the SODAR. This noise will be observed at all range gates.

The SODAR records the time series of the baseband I and Q signals. For the nominal 60-m maximum range, the round trip distance is 120m. If the pulsed energy travels at the speed of sound $c = 340$ m/s (at 20 degrees Celsius), then the time delay between pulses (including the transmitted 30-msec pulse) is roughly $\Delta t = 0.45$ s. Depending on processing time, which can decrease the number of samples, there are approximately 412 samples per pulse in the examples below.

Figure 1 shows sample raw time series scattering amplitude data (magnitude of I,Q vector) for 190 seconds; a darker point represents higher amplitude. During this period a Boeing 737 passed the sodar and its corresponding noise and vortex are noted. Note that, to compensate for the reduction in turbulence scattering with altitude, the sodar multiplies the scattering amplitude by a linear ramp starting at the beginning of the transmitted pulse. This ramp leads to noise signals that increase for higher range. The bands across the bottom of the figure are the transmitted pulse and ground clutter, which do not correspond to useful data. The vertical, black hashed lines at the left are the noise generated by the arriving aircraft and its corresponding vortex, which appears elliptical, located at approximately 56 seconds. Enhanced scattering is noted near the vortex core. Additionally, two other aircraft are noted with their corresponding noise bands.

IV. Algorithms for Detecting and Measuring Wake Vortices

A. Phase 1—Range Gates

The first phase of processing involves generating spectra from overlapping range gates. The following steps are performed:

1. The first 29 samples include ground clutter and side lobe energy, and are therefore ignored.
2. Starting with the 30th sample, the next 32 points are selected for the first range gate. They are multiplied by a 32 point Hanning window, as shown in Figure 2a. The time-series, plotted in red, shows areas of higher returns at the beginning, middle and end of the 32 points. When the Hanning Window, plotted in green, is applied to the time-series amplitude (plotted in red), the resultant, plotted in blue, illustrate that the end points of the time-series are attenuated. The window serves to broaden the spectra while attenuating side lobes.
3. The I and Q time series are then converted to spectra using an FFT. Figure 2b shows the same example in the frequency domain. The blue and red plots show the signal spectrum with and without the Hanning window. With the window the spectrum is smoother and the main peak is better defined. The green plot shows the spectrum of the Hanning window.

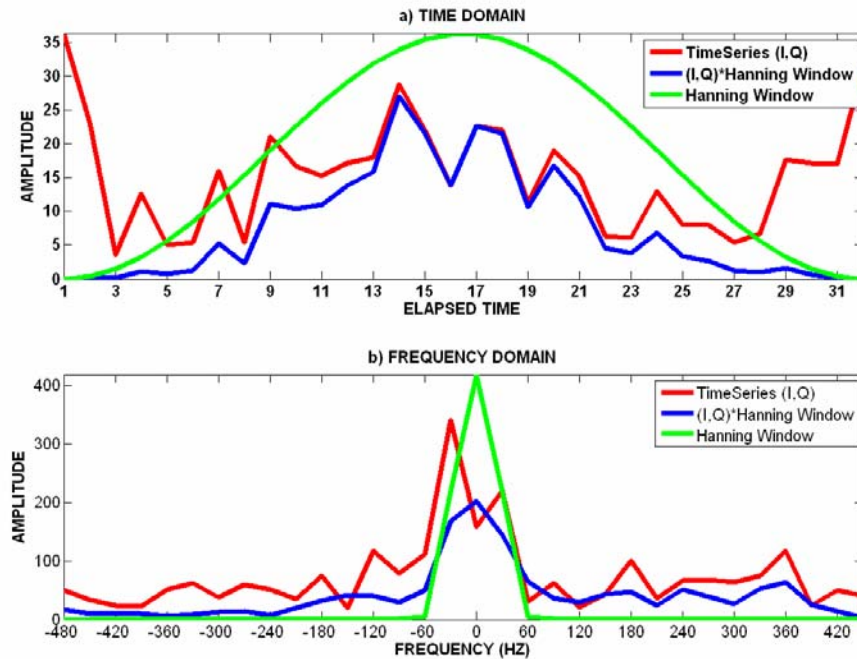


Figure 2 Thirty two time series points: Raw data (red), Multiplied by 32-point Hanning (blue), and Hanning window alone (green): a) time domain and b) frequency domain.

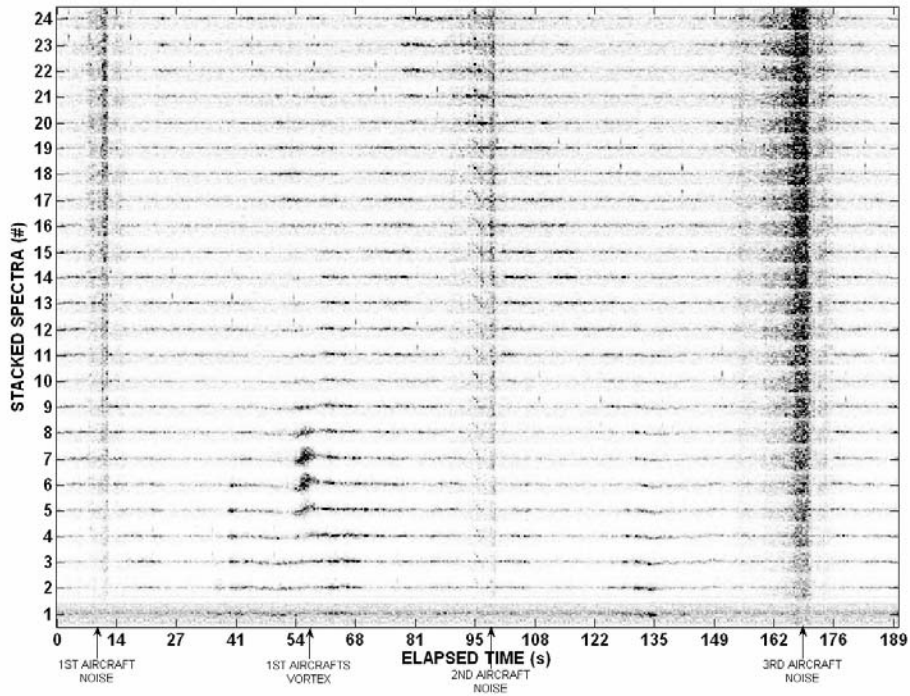


Figure 3 Stacked Spectra, illustrating noise from three arriving aircraft and a wake vortex associated with the first arrival, a Boeing 737.

4. The starting point is incremented by 15 points and the processing is repeated starting at step 2. The process is stopped when a range gate would have less than 32 points. For 412 samples, spectra are generated for 24 range gates.

This process is repeated for each pulse until the entire data period is completed.

The spectra can be plotted in a similar fashion as the amplitude was in Figure 1. Figure 3 illustrates the 24 stacked spectra for the same 190 seconds of data in Figure 1. Again, the noise generated from three arriving aircraft is noted. The vortex core location shows up as a maximum Doppler spread in Range Gates 6 and 7 at time 56 seconds.

The passage of the vortex core is signaled by the change in sign of the Doppler shifts. The stronger scattering from the wake is observed from time 40 to perhaps 75 seconds. At stacked spectrum 6, the sign starts zero at 40 seconds, shifts negative at time, passes through zero at time, and shifts positive at time. This is the characteristic Doppler signature (updraft followed by a downdraft) associated with the first vortex to reach a sodar antenna. The second vortex to reach a sodar antenna has the opposite sign.

B. Phase 2—Vertical Velocity Field

The next processing phase identifies some characteristic of spectrum as the best estimate of the vertical velocity component of the range gate. A number of options are possible:

1. The wind SODAR algorithm finds the best 5-point fit to a peak in the spectrum. This algorithm is less appropriate for the broad spectrum near a vortex core.
2. The traditional vortex SODAR algorithm calculated the first and second moments of the power spectrum. These values can be strongly influenced large-doppler noise.
3. The algorithm selected calculates the median Doppler frequency shift of the power spectrum. Interpolation is done between the two points nearest the median value.

Equation 1.1 allows for finding the velocity measurement v from Doppler shift Δf .

$$v = -(20.05 * \sqrt{273 + C}) * (\Delta f / 2f) \text{ m/s} \quad (1.1)$$

where C is the temperature in degree Celsius, and f is the transmit frequency of the SODAR. For the above example, at 20 degrees Celsius, we calculate $v = -1.46$ m/s.

The total signal power can be useful in looking at the overall energy or amplitude in a spectral segment. Every range gate therefore has the signal amplitude determined from the following equation:

$$A = \sqrt{\sum_{i=1}^{32} X_i^2} \quad (1.2)$$

where X is the spectral amplitude at bin i .

The signal-to-noise ratio (SNR) can help determine noisy or bad data. Data associated with low SNR values indicated that the noise is greater than the signal and should not be used. Since $P_{1/2}$ is on average associated with one of the middle 16 Doppler bins, we can consider this the signal S_i , the remaining outer bins, bins 1-to-8 and 25-to-32 are the noise S_N . The equation for SNR is:

$$\text{SNR} = S_i / S_N \quad (1.3)$$

For the above example $\text{SNR} = 3.02$.

Equations 1.1 – 1.3 are repeated on all data in the specified time period, typically 190 s. For each 32 point spectral segment, which again is the FFT of 32 samples of I and Q measurements incremented by 15 samples consecutively, we obtain one point measurement. These single point measurements correspond to the velocity at a particular range gate. Therefore for each pulse we obtain 24 range-gate measurements, with a range-gate spacing (15 samples) of 2.65 m. Figure 5a shows vertical velocity profiles of 190s. The noise associated with the first aircraft can be seen at 12s and its corresponding first wake vortex at 56s. The image of the velocity profile shows the characteristic vortex signature. As the clockwise rotating vortex passes through the antenna, its vertical velocity

will have a positive sign (red) indicating the wake is moving away from the sodar (up). The vortex continues to pass through the antenna and its tangential velocity decreases towards zero. This means that all of the tangential velocity is in the horizontal direction, and the SODAR can not measure it. As rotation continues the velocity becomes increasingly negative (blue) indicating the vortex is moving towards the SODAR (down).

Figure 5b shows the image of the signal amplitude for each velocity profile, noted are the noise spikes of three arriving aircraft, which appear as higher intensities. The log base 10 of the data set was calculated to better show the variance in color or signal. The vortex discussed above also appears as a higher intensity, indicating a signal. The final plot figure 5c shows the $\log_{10}(\text{SNR})$ for the velocity profile. The noise spikes from the aircraft as would be expected show low SNR, this is due to the fact that noise interference is received directly from the aircraft rather than returns of eddies. The vortex however shows up as a high SNR in comparison to the aircraft noise.

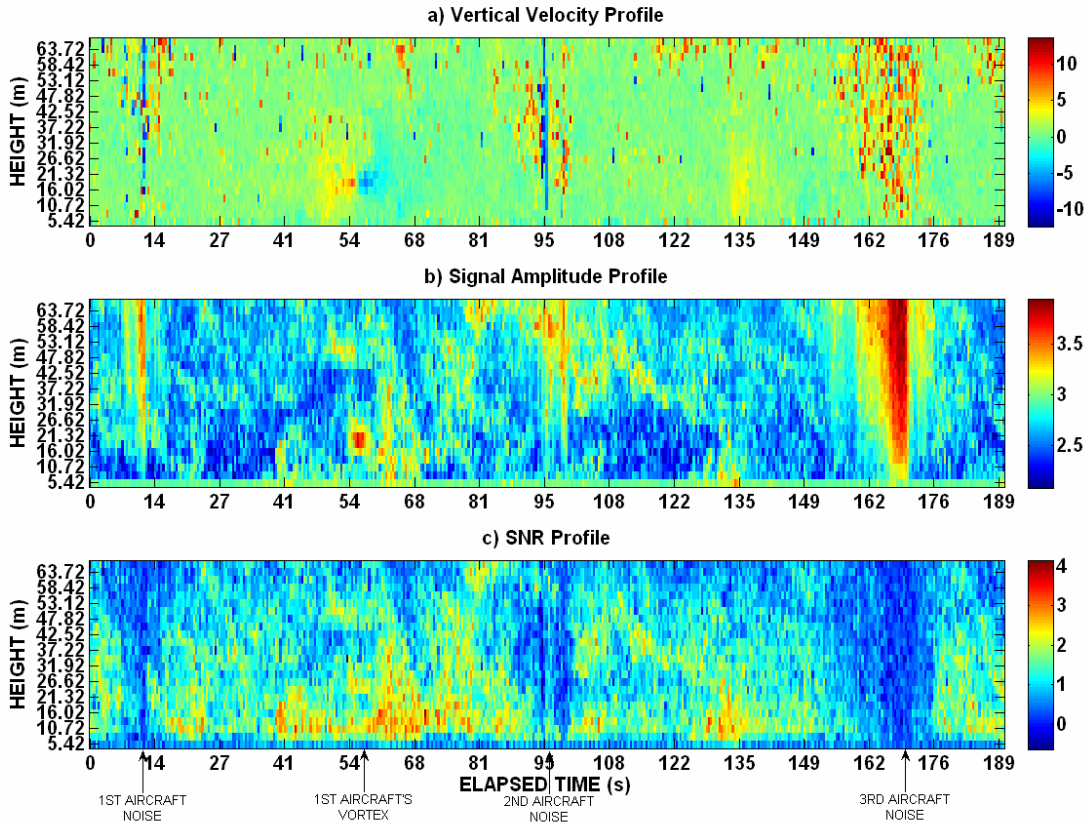


Figure 5 a) Vertical Velocity Profiles, b) Signal Amplitude Profiles, c) SNR Profiles.

C. Phase 3—Vortex Location

A correlation method is used to locate the two wake vortices in the vertical flow field measured by the SODAR. The vertical flow field is correlated with a function shaped like the expected vortex velocity field. Traditionally a correlation method multiplies the measurements by the expected signature. However, if the signature is a constant, then the multiplications are actually additions. The simple vortex shape is a single-cycle square wave in time, each segment of which had a distance of 10 meters. It is positive for 10 meters before the vortex core arrives at the SODAR and negative for 10 meters after the core arrives. Knowing the aircraft passage time, this correlation function must expand in time as the vortex takes longer and longer to reach the SODAR. The corresponding vertical extent of the correlation function would be 20 meters, or many range gates. In practice, only a single range gate was used in the vertical direction. A number of additional features are applied to make this method more robust:

1. Points with signal-to-noise ratio below a threshold are not included.
2. The center of the correlation function can be located on a data point or between data points.

3. The value of the correlation is normalized to the number of points summed to give a number equal to the mean velocity over the 10-meter range. This approach also permits comparison of correlation values with different time lengths.
4. The portions of the correlation function before and after the vortex core are summed separately and both are required to make the same sign and comparable magnitudes to the total correlation. The contributions of the two sides must be comparable to within a factor of 4. This requirement prevents a single-sided shift in vertical velocity to be identified as a vortex. Such shifts can be generated by ambient noise and are always located on the edge of the other vortex.
5. The most positive and negative correlation values represent the arrival times of the first and second vortices to reach the sodar.
6. For vortex detection the magnitude of the correlation value must be greater than a specified minimum value.

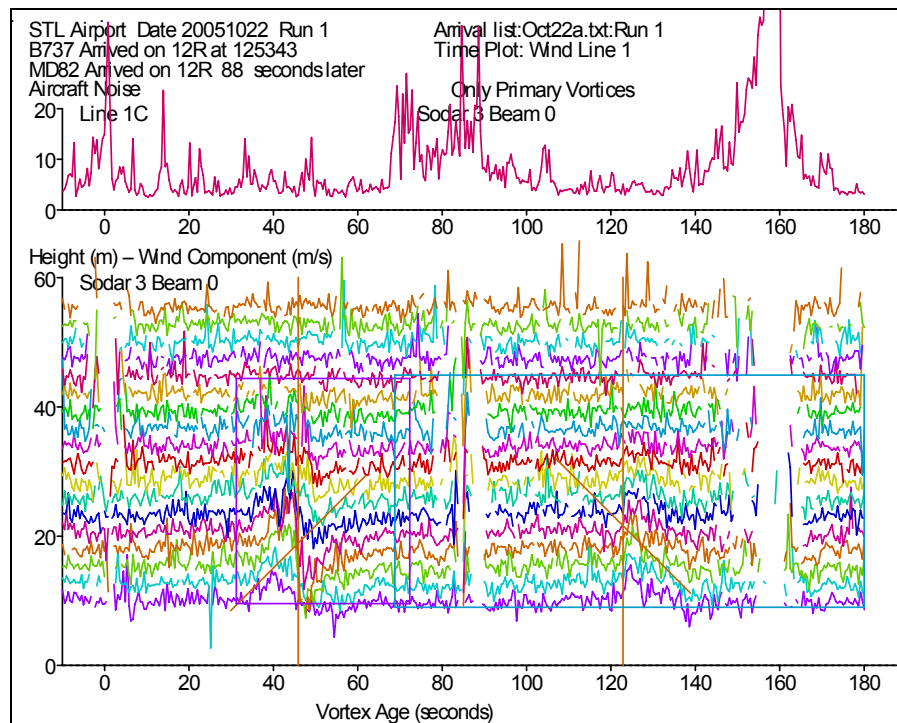


Figure 6 Vortex Detections for Sodar Located 97 m from Centerline of Runway 12R: Top: Signal intensity in highest range gate; Bottom: vertical velocity vs. wake age for all range gates.

The output of the vortex detection algorithm is the arrival time and of one or both vortices. Figure 6 illustrates some of the features of the vortex detection algorithm. Note that, in contrast to Figure 5, zero time in Figure 6 is the time the first aircraft passed the sodar antenna. The bottom plot of Figure 6 shows the same vertical velocity data as the top plot of Figure 5, but with a line plot for each range gate rather than a color plot. A positive velocity corresponds to an updraft. The top plot of Figure 6 shows the signal intensity in the top range gate (top line of middle plot in Figure 5); noise spikes are noted at the arrival times of the three aircraft, as well as at other times. In Figure 6 both vortices were detected; the time of detection is marked by a vertical orange line and the range gate of detection is marked with a diagonal orange line:

1. The first vortex (updraft followed by downdraft) was detected at wake age 46 seconds with a correlation value of -10.6 m/s. The fit, described in the next section was successful for this vortex. Figure 7 (left) shows an expanded view of the flow field around this vortex. The velocity field is quite noisy.
2. The second vortex (downdraft followed by updraft) was detected at wake age 123 seconds with a much lower correlation value of 2.22 m/s. This weak vortex detection long after the arrival of the next aircraft was probably not a real vortex but an artifact. One indication of an invalid detection is that the fit did not converge for this vortex detection. A non-converging fit was found to be a good method for automatically rejecting invalid detections where the flow field is not well described by theory.

The two rectangular boxes in Figure 6 show the ages and range gates searched for the two vortices. Both were detected near the middle of their search zones. The search zone for the first vortex was narrowed by the detection of the vortex by the collocated Windline. The Windline and SODAR (larger X) lateral positions are shown in the bottom, left plot of Figure 7. The two sensors gave consistent vortex locations. Note that the straight line in this plot is a fit to the windline data.

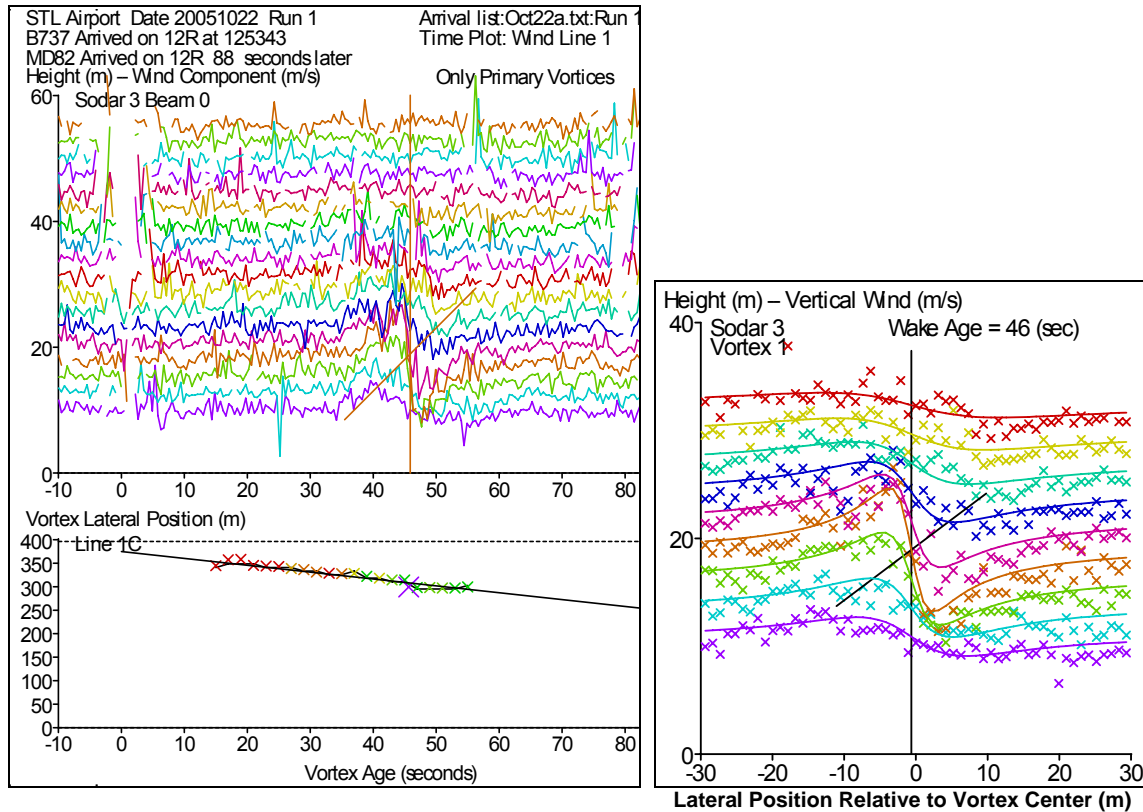


Figure 7 Left: Expanded sodar vertical velocity data (top) and lateral position from Sodars and Windline (bottom); Right: Vertical velocity profiles from fit (line) and measurements (points)

In recent practice often one and no more than three vortex SODARs have been installed in an array. The positions in between have been filled with windline and/or pulsed LIDAR measurements. As suggested above, the time search region for SODAR vortex detection can be narrowed by knowing the crosswind or the vortex track from another sensor – which in the case of St Louis, being provided either by the Windline or from the airport centerline field wind, otherwise also known as the Automated Surface Observation System (ASOS). Alternatively, it may also be provided by a nearby SODAR operating in the traditional wind mode.

D. Phase 4—Vortex Circulation

An approximate vortex lateral transport speed is adequate for the vortex location algorithm but can be a problem for calculating vortex circulation that is roughly proportional to the transport speed. Several transport speed alternatives are possible:

1. The earlier SODAR array measurements used the arrival times at successive SODAR antennas to calculate accurate transport speeds. This method is not applicable to one or two SODARs over a large transport distance.
2. The time of vortex detection can be used to derive an assumed constant transport speed from an assumed initial vortex location. This is the default method.
3. Ambient crosswind measurements could be used to estimate the transport speed.
4. Transport measurements from other wake sensors could be used to estimate the transport speed.

Several alternative circulation algorithms are also possible:

1. The tangential vortex velocity profile can be taken from the range gate with the maximum correlation value. The circulation can be calculated as an average between selected core radii, e.g., 10 to 20 meters. The selected core radii should be greater than the spatial resolution of the sodar. This method was used for the earlier sodar measurements and seemed to give reliable results. Recent commercial SODAR results seem less reliable than method 3 below.
2. The velocity field in the vicinity of a vortex (e.g., ± 4 range gates and ± 30 m lateral position as in the right plot of Figure 7) can be fitted to the parameters of core radius (r_c) and total circulation (Γ_∞) using a model for the vortex velocity profile. In this case the core radius is not the real core size but rather the resolution of the sodar.
3. In some cases the core radius given by the fit method is unrealistically large and leads to unrealistic circulation values. A more reasonable value that better matches the data used for the fit can be obtained by integrating the fitted tangential velocity profile from 10 to 20 meters.

The vortex tangential velocity model used for the fit is:

$$v(r) = r\Gamma_\infty / 2\pi(r^2 + r_c^2) \quad (1.4)$$

The initial estimates for the vortex parameters:

1. Height = height of range gate with maximum correlation,
2. Lateral position = zero at time of maximum correlation,
3. Γ_∞ = factor times maximum correlation, and
4. r_c = fixed value (10 m).

These parameters are varied systematically to minimize the sum of the squares of the differences between the measured and calculated vertical velocity field, excluding points with poor signal-to-noise ratio. If the fit does not converge in a reasonable number of steps, the fit is abandoned. The right plot of Figure 7 compares the fitted and measured vertical flow field of the vortex. Note that the assumed transport speed is used to change the measured time series flow field above the sodar (top, left of Figure 7) to the spatial flow field (right of Figure 7), assuming that the flow field changes little as it passes over the sodar.

Table 1 shows the parameters derived from the sodar measurements for the sample case. The fitting process changes the vortex age by only 0.3 seconds but did not change the vortex height. The three alternative circulation parameters were fairly close together for this case.

Table 1. Parameters from Sodar Processing

Parameter	Value
Vortex	First
Correlation Age	45.9 sec
Fitted Age	45.6 sec
Correlation Value	-10.58 m/s
Correlation Height	18.9 m
Fitted Height	18.9 m
Transport Speed	2.33 m/s
Fitted Core Radius	3.11 m
Fitted Circulation	-217.7 m ² /s
10-20-m Average Circulation from One Range Gate	-199.8 m ² /s
10-20-m Average Circulation from Fit	-207.7 m ² /s

V. Conclusions

A commercial wind SODAR can be successfully adapted to the measurement of aircraft wake vortices. As was found in earlier SODAR measurements of wake vortices, some human validation was required to assure that all vortex detections are valid. The validation step was simplified by the observation that the least-squares fit does not converge for most false vortex detections.

Recent SODAR measurements have been used successfully to validate vortex measurements from a pulsed LIDAR system. Because of its much greater spatial coverage, the pulsed LIDAR has generally then considered as the preference over vortex SODARs or Windlines for collecting large datasets on wake behavior in-ground-effect. However, specific topological consideration as well as the clearance needed for LIDARs meant that it is not always possible to use optical sensors exclusively in an airport measurement campaign. As such, an array of vortex SODARs provides an attractive and only alternative for both tracking and quantifying the circulation evolution of the vortices in-ground-effect.

The possible capability of a vortex SODAR to use core reflections to measure wake vortex core sizes is perhaps one of the most intriguing possibilities for future wake vortex studies. Vortex core size measurements has implications for validating vortex decay models and perhaps even for estimating encounter hazards for very large aircraft.

Acknowledgements

The study is sponsored jointly by the Federal Aviation Administration (FAA) and the National Aeronautics and Space Administration (NASA). The authors wish to express their appreciation for the technical guidance of George Greene of the FAA. Moreover, the authors wish to express their appreciation to Wayne Bryant of NASA's Airspace Systems Program of the Aeronautics Research Mission Directorate, for ensuring that the work focused on addressing issues that are of both fundamental and practical interests. Finally, the authors also acknowledge the encouragement and support of Robert Rudis and Michael Geyer of the USDOT Volpe Center.

References

- ¹Burnham, D., Sullivan, T., and Wilk, L., "Measurements of Wake Vortex Strength by Means of Acoustic Back Scattering," *Journal of Aircraft*, Vol. 10, No. 11, 1976, pp. 889-894.
- ²Bradley, S. G., "Validation of Sodar Real-Time Sensing and Visualisation of Wake Vortices," Proceedings of the 12th Conference on Aviation Range and Aerospace Meteorology, Atlanta, GA., January 30, 2006 – February 2, 2006.
- ³Bradley, S. G., von Hünerbein, S., and Underwood, K., "Operational Reliability and Accuracy of SODARs in Wing Vortex Characterization," Proceedings of the 12th Conference on Aviation Range and Aerospace Meteorology, Atlanta, GA., January 30, 2006 – February 2, 2006.
- ⁴Fiduccia, P. C., Bryant, W., and Lang, S., "FAA/NASA Wake Turbulence Research Program," *Journal of ATC*, Vol. 46, No. 1, January-March 2004, pp. 17-21.
- ⁵Gertz, T., Holzäpfel, F., Bryant, W., Köpp, F., Frech, M., Taffermer, A., and Winckelmans, G., "Research Towards a Wake-Vortex Advisory System for Optimal Aircraft Spacing," *Comptes Rendus Physique*, Vol. 6, 2005, pp. 501-523.